

## SECTION LISTING

## BROWSE VOLUME

Year Range: 2000-2009

Volume 94 2009

Issue 23 8 Jun 2009 **PARTIAL ISSUE**

Issue 22 1 Jun 2009

Issue 21 25 May 2009

Issue 20 18 May 2009

Issue 19 11 May 2009

Issue 18 4 May 2009

Issue 17 27 Apr 2009

Issue 16 20 Apr 2009

Issue 15 13 Apr 2009

Issue 14 6 Apr 2009

Issue 13 30 Mar 2009

Issue 12 23 Mar 2009

Issue 11 16 Mar 2009

Issue 10 9 Mar 2009

Issue 9 2 Mar 2009

Issue 8 23 Feb 2009

Issue 7 16 Feb 2009

Issue 6 9 Feb 2009

Issue 5 2 Feb 2009

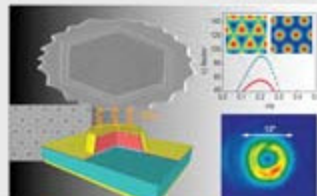
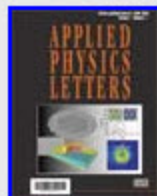
Issue 4 26 Jan 2009

1 June 2009

Volume 94, Issue 22, Articles (22xxxx)

[Search Issue](#) | [Previous Issue](#) | [Next Iss](#)

[TOC Alert](#) [RSS](#)



Cover image from Gangyi Xu, Virginie Moreau, Yannick Chassagneux, Adel Bousseksou, Raffaele Colombelli, G. Patriarcho, G. Beaudoin, and Sagnes, *Appl. Phys. Lett.* **94**, 221101 (2009).

[Enlarge the Image](#) | [Read the Article](#)

SELECTED: [Export Citations](#) | [Show/Hide Summaries](#) | [Add to MyArticles](#) | [Email](#)

[Add](#) [View](#)

0

## LASERS, OPTICS, AND OPTOELECTRONICS

TOP ↑

### Surface-emitting quantum cascade lasers with metallic photonic-crystal resonators

Gangyi Xu, Virginie Moreau, Yannick Chassagneux, Adel Bousseksou, Raffaele Colombelli, G. Patriarcho, G. Beaudoin, and I. Sagnes

*Appl. Phys. Lett.* **94**, 221101 (2009) (3 pages)

Online Publication Date: 1 June 2009

Full Text: [HTML](#) | [Sectioned HTML](#) | [PDF](#) (428 kB)

+ [Show Abstract](#)

+ [Show PACS](#)

### Exact surface plasmon dispersion relations in a linear-metal-nonlinear dielectric structure of arbitrary nonlinearity

Haiping Yin, C. Xu, and P. M. Hui

*Appl. Phys. Lett.* **94**, 221102 (2009) (3 pages)

Online Publication Date: 1 June 2009

Full Text: [HTML](#) | [Sectioned HTML](#) | [PDF](#) (166 kB)

## Carbon nanotube and conducting polymer dual-layered films fabricated by microcontact printing

Jin Woo Huh,<sup>1,a)</sup> Jin Wook Jeong,<sup>1</sup> Jin Woo Lee,<sup>1</sup> Sang-Il Shin,<sup>1</sup> Jae-Hong Kwon,<sup>1</sup> Jinnil Choi,<sup>1</sup> Ho Gyu Yoon,<sup>2</sup> Gyeong-Ik Cho,<sup>3</sup> In-Kyu You,<sup>3</sup> Seung-Youl Kang,<sup>3</sup> and Byeong Kwon Ju<sup>1,b)</sup>

<sup>1</sup>Department of Electrical Engineering, Korea University, Seoul 136-713, Republic of Korea

<sup>2</sup>Department of Materials Science and Engineering, Korea University, Seoul 136-713, Republic of Korea

<sup>3</sup>Convergence Components & Materials Research Laboratory, Electronics and Telecommunications Research Institute, Daejeon 305-700, Republic of Korea

(Received 21 December 2008; accepted 26 April 2009; published online 5 June 2009)

We report carbon nanotube/conducting polymer dual-layered film (CPDF) electrodes fabricated by microcontact printing for flexible transparent electrodes of organic thin film transistors (OTFTs). The CPDFs show  $\sim 1000 \text{ } \Omega/\text{sq}$  surface resistivity and  $\sim 93\%$  transmittance at an extremely low loading of single-walled carbon nanotubes, and can be self-aligned with a precision of  $20 \text{ } \mu\text{m}$ . The CPDFs are applied as the source and drain electrodes in OTFTs without any supplementary alignment process, which leads to a mobility and a current on/off ratio of approximately  $0.02 \text{ cm}^2 \text{ V}^{-1} \text{ s}^{-1}$  and  $\sim 10^4$ , respectively. © 2009 American Institute of Physics.

[DOI: 10.1063/1.3137185]

In recent years, carbon nanotubes (CNTs) have attracted much attention for their use as a polymer-composite filler in flexible transparent electrodes.<sup>1,2</sup> In order to realize these composites, it is important that the content of CNT in the composite should be as low as possible for sufficient transparency, and the nanotubes need to be homogeneously dispersed in the polymer with networking for high conductivity. By selective localization of all the CNTs at the surface of the polymer rather than full dispersion within the whole polymer volume, a dual-layered film system of individually coated CNT and polymer layers can be used to obtain good optoelectrical properties of the film. This concept of selective localization has been previously illustrated<sup>3,4</sup> as an efficient strategy for achieving a very low percolation threshold.

When patterning dual-layered film, the key points to be considered are as follows: (1) Each material should be aligned without any additional processing, and (2) the pattern should be developed by a solution process appropriate for fabricating flexible organic devices. To date there have been few studies on fabrication methods, which satisfy the soluble and multilayer-alignable process on the patterns of dual-layered films and on their application as flexible transparent electrodes. This paper introduces a CNT/conducting polymer dual-layered film (CPDF) with a considerably low loading level of CNT, and microcontact printing (MCP)<sup>5-7</sup> using a self-assembled monolayer (SAM)<sup>6,7</sup> as a patterning method. The potential application of the CPDF as a transparent electrode for organic thin film transistor (OTFT) is also demonstrated.

The conducting polymer used here was a dispersed poly(3,4-ethylenedioxy-thiophene),<sup>8</sup> doped with poly(styrenesulfonic acid) (PriMet-S, DPI Solutions, Inc.) with a surface resistivity of  $\sim 4000 \text{ } \Omega/\text{sq}$  for a film of  $1000 \text{ } \text{Å}$ . The polymer solution was spin coated at 3000 rpm and dried at

$90 \text{ } ^\circ\text{C}$  to form a film of this thickness. The single-walled carbon nanotubes (SWNTs), synthesized by an arc-discharge process and purified with acid (ASP-100F, Iljin Nanotech Co., Ltd.), were dispersed in water with the aid of 1 wt % sodium dodecyl sulfate under pulse sonication for 2 h. The aqueous SWNT solution was spin casted on a conducting polymer film coated substrate.

Octadecyltrichlorosilane (OTS) (Aldrich) was used as the SAM material to guide the patterns of the CNT and the polymer. Using the SAM technology, the CPDF source and drain electrodes for OTFT were fabricated as follows [see Fig. 1(a)]: (1) 10 mM of OTS was diluted with hexane (Aldrich) and spin coated on the polydimethylsiloxane (PDMS) stamp,<sup>9</sup> which was then contacted on the UV-cleaned substrate for 30 s; (2) after the OTS stamping, the conducting polymer solution was spin coated onto the OTS-SAM pre-patterned substrate and then dried; and (3) the aqueous CNT solution is spin cast on the polymer; and then (4) the active

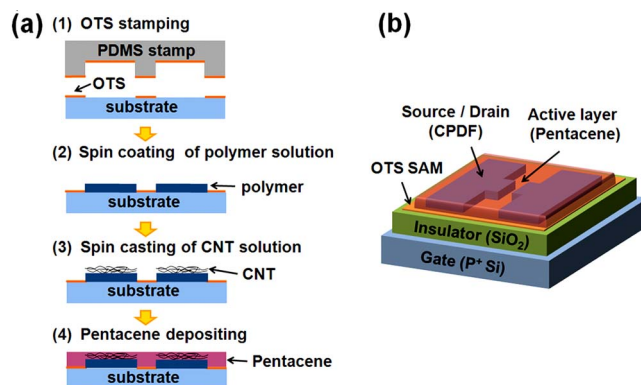


FIG. 1. (Color online) (a) Schematic depicting process of CPDF electrodes patterning for OTFT using MCP. (b) The structure of OTFT implemented with CPDF electrodes, which are introduced to a doped Si substrate, with a 300 nm thermally grown oxide layer used as the bottom gate. A 70 nm thick active layer of pentacene is evaporated on the defined source and drain electrodes at a rate of around  $0.3 \text{ } \text{Å}/\text{s}$ .

<sup>a)</sup>Electronic mail: jwhuh@korea.ac.kr.

<sup>b)</sup>Author to whom correspondence should be addressed. Electronic mail: bkju@korea.ac.kr.

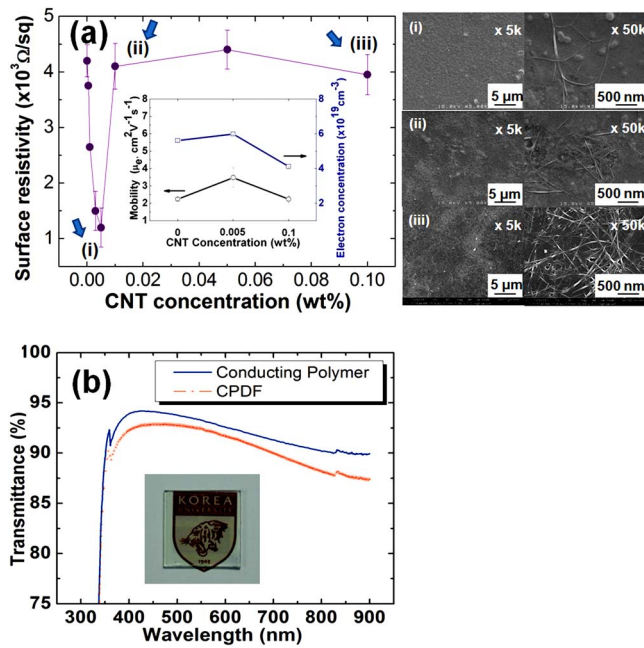


FIG. 2. (Color online) (a) Surface resistivity of CPDF as a function of CNT concentration (0, 0.0001, 0.001, 0.003, 0.005, 0.01, 0.05, and 0.1 wt %) and SEM images of CPDF at the CNT concentrations of (i) 0.005, (ii) 0.01, and (iii) 0.1 wt %. [Inset: conduction electron mobility of the CPDF obtained by a Hall effect measurement system (Ecopia, HMS-1000) over the area of  $0.5 \times 0.5$  cm<sup>2</sup>.] (b) Transmittance of the CPDF with thickness of 1000 Å at 0.005 wt % CNT concentration. (Inset: a photograph of CPDF on glass located above the institutional logo).

layer of pentacene was evaporated on the CPDF source and drain electrodes.

The structure of the OTFT is shown in Fig. 1(b), where the CPDF electrodes have channel length and width of 20 and 1000 μm, respectively.

Figure 2(a) shows the change in surface resistivity of the SWNT spin-cast side of the CPDF with a thickness of ~1000 Å with the CNT concentration. The resistivity of the film decreases dramatically to ~1000 Ω/sq at an extremely low loading of 0.005 wt %. This level is less than 1/5 of the magnitude of ~0.026 wt % reported as the very low percolation threshold<sup>10</sup> in the conventional composites of the CNTs dispersed in a polymer matrix.<sup>11,12</sup> However, it is noticeable that the resistivity drastically increases again as the CNT concentration increases to that of the conducting polymer itself, differing with the typical percolation behavior of the conventional composites.

This phenomenon can be explained by the change in the contact resistance between the SWNTs. The scanning electron microscope (SEM) images in Fig. 2(a) [(i)–(iii)] show the degree of impregnation of SWNTs into the conducting polymer. The aqueous CNT solution swells the conducting polymer surface, so that the CNTs would smoothly be impregnated into the water-swollen polymer during spin casting. At 0.005 wt %, as seen in Fig. 2(a)(i), the nanotubes are better impregnated into the polymer than the other CNT concentration CPDFs, without any excess tubes exposed on the surface, and are uniformly dispersed to form a conductive network on the polymer layer. In addition, it can be expected to have  $\pi$ - $\pi$  bonding between the styrene moiety in the conducting polymer and the hexagon in the CNT. These may cause minimal contact resistance between the SWNTs, and enhancement of the electrical conductivity approaching that

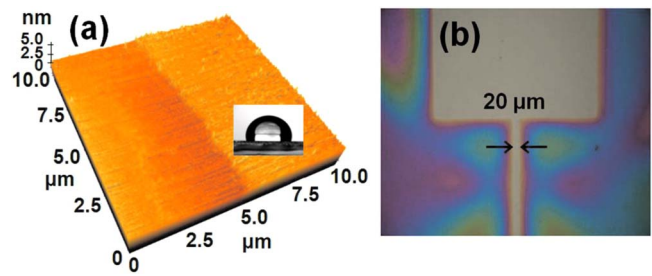


FIG. 3. (Color online) (a) AFM image ( $10 \times 10$  μm<sup>2</sup>) of OTS-SAM pattern on SiO<sub>2</sub>/Si substrate. (Inset: contact angle after the OTS-SAM treatment). (b) Microimage of the pattern of CPDF for source and drain electrodes.

of SWNTs themselves at the surface of the CPDFs. At concentrations greater than 0.01 wt %, there exist CNT bundles, which are not far enough to be impregnated into the polymer. These bundles are separated in a microscale rather than being connected with each other on the polymer surface, as shown in Figs. 2(b) [(ii) and (iii)], indicating that the electrical conducting path in the CPDF may be disturbed by the separated CNT agglomeration. This is supported by previously reported results<sup>1</sup> in which the agglomerated microstructure, at high nanotube loading in spin-coated films, leads to a drop in conductivity.

The electron mobility in the CNT cast side of the CPDF measured by van der Pauw's method,<sup>13</sup> as shown in the inset of Fig. 2(a), confirms the SEM results, showing that the mobility of the electrons in the film with 0.005 wt % are higher than those of other cases, which agrees with the trend of the surface resistivity. This reveals that, although the amount of CNTs is very low, efficient electrical conduction in the CPDF could be achieved at around 0.005 wt % by minimizing the contact resistance through the impregnation of the CNTs into the polymer, and by helping the mobility of free electrons via networking.

The electron mobility in the dual-layered film depends on the side with higher conductivity; if the measured surface has higher conductivity than the opposite side, the mobility is hardly affected by the electrical properties of the opposite side, and vice versa. Since the electrical properties of the SWNT cast side in the CPDF were measured, the data of mobility and electron concentration would be close to the value of the SWNT rich side itself.

Low loading of the CNTs results in high transparency and Fig. 2(b) shows the transmittance of the CPDF with the resulting thickness of 1000 Å by adding 0.005 wt % of CNTs. The value in the visible spectrum region is 90%–93%, which is comparable to the transmittance of the conducting polymer film without adding CNTs, and meets the requirement of the transparent electrodes.

Figure 3(a) shows the atomic force microscope (AFM) image of the OTS pattern, prepared over the SiO<sub>2</sub>/Si substrate using the PDMS stamp. The thickness of the pattern is approximately 2.5 nm, representing one monolayer of OTS molecules. The contact angle is 105°, as shown in the inset, which means that the formation of CPDF would be prevented on this pattern due to its hydrophobic behavior. Figure 3(b) shows the source and drain electrodes with sharp edges at intervals of 20 μm between them, fabricated at the CNT loading of 0.005 wt % with a thickness of 1000 Å. Considering that the current limit of high resolution patterning processes, such as inkjet printing, is about 20 μm, this

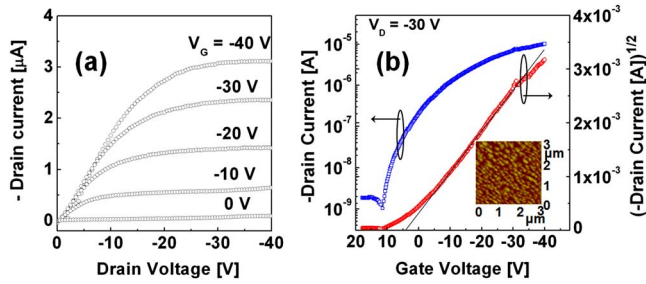


FIG. 4. (Color online) (a) Output curve and (b) transfer curve of a pentacene OTFT having CPDF source and drain electrodes. The output and transfer curves are obtained by a semiconductor characterization system (Keithley SCS 4200) in a dark box. [Inset (b): AFM image ( $3 \times 3 \mu\text{m}^2$ ) of morphology of the pentacene in channel.]

shows that MCP, using the OTS-SAM pattern, can be an effective method of obtaining a fine pattern of CPDF without additional alignment.

The characteristics of the OTFT implemented with source and drain electrodes of the CPDF are shown in Figs. 4(a) and 4(b). Figure 4(a) shows that the output curve has good linear/saturation behavior at the operating voltages and the curve clearly shows typical *p*-type accumulation mode and pinch off. As shown in Fig. 4(b), the field-effect hole mobility, extracted from the transfer curve at a drain voltage of  $-30$  V, is  $0.02 \text{ cm}^2/\text{Vs}$  at the saturation region, the threshold voltage is  $4$  V, and the current on/off ratio is  $\sim 10^4$  with a subthreshold swing of  $1.58$  V/decade. This performance of the device with the CPDF electrodes is comparable to that of those devices with Au electrodes.<sup>14</sup> This verifies the contact between the CPDF electrode and pentacene is well formed, which is consistent with recently reported findings for the CNT-based transistors.<sup>15</sup> In addition, this confirms that the OTS-SAM surface treatment of  $\text{SiO}_2$  prior to pentacene deposition improves the device characteristics due to the tight molecular packing of pentacene in the channel by reducing the grain size to  $\sim 0.2 \mu\text{m}$ , as shown in the inset of Fig. 4(b).<sup>14,16</sup>

In summary, the CPDF is easily fabricated with a very low loading of the CNTs at  $0.005 \text{ wt } \%$ , and has been applied as the source and drain electrodes in OTFTs, without any

additional alignment processes, by the MCP with a precision of  $20 \mu\text{m}$ . The electrodes, with  $\sim 1000 \Omega/\text{sq}$  surface resistivity and  $\sim 93\%$  transmittance, led to the mobility and on/off ratio of approximately  $0.02 \text{ cm}^2 \text{ V}^{-1} \text{ s}^{-1}$  and  $\sim 10^4$ , respectively. These results indicate that the CPDF is a promising alternative for flexible and highly transparent electrodes, and that the MCP, using SAM technology, can be an efficient process for fabricating CPDF electrodes.

This work was supported by the National Research Laboratory (NRL) program (Grant No. ROA-2007-000-20111-0) of the Ministry and Science of Technology and the IT R&D program (Grant No. 2008-F-024-02, Development of Mobile Flexible IOP platform) of MKE in Korea.

- <sup>1</sup>R. H. Schmidt, I. A. Kinloch, A. N. Burgess, and A. H. Windle, *Langmuir* **23**, 5707 (2007).
- <sup>2</sup>V. Bocharova, A. Kiriy, U. Oertel, M. Stamm, F. Stoffelbach, R. Jerome, and C. Detrembleur, *J. Phys. Chem. B* **110**, 14640 (2006).
- <sup>3</sup>F. Gubbels, S. Blacher, E. Vanlathem, R. Jerome, R. Deltour, F. Brouers, and Ph. Teyssie, *Macromolecules* **28**, 1559 (1995).
- <sup>4</sup>F. Gubbels, R. Jerome, E. Vanlathem, R. Deltour, S. Blacher, and F. Brouers, *Chem. Mater.* **10**, 1227 (1998).
- <sup>5</sup>M. A. Meitl, Y. Zhou, A. Gaur, S. W. Jeon, M. L. Usrey, M. S. Strano, and J. A. Rogers, *Nano Lett.* **4**, 1643 (2004).
- <sup>6</sup>V. V. Tsukruk, H. Ko, and S. Peleshanko, *Phys. Rev. Lett.* **92**, 065502 (2004).
- <sup>7</sup>S. G. Rao, L. Huang, W. Setyawan, and S. Hong, *Nature (London)* **425**, 36 (2003).
- <sup>8</sup>J. W. Huh, Y. M. Kim, Y. W. Park, J. H. Choi, J. W. Lee, J. W. Lee, J. W. Yang, S. H. Ju, K. K. Paek, and B. K. Ju, *J. Appl. Phys.* **103**, 044502 (2008).
- <sup>9</sup>A. Kumar and G. M. Whitesides, *Appl. Phys. Lett.* **63**, 2002 (1993).
- <sup>10</sup>Y. J. Kim, T. S. Shin, H. D. Choi, J. H. Kwon, Y.-C. Chung, and H. G. Yoon, *Carbon* **43**, 23 (2005).
- <sup>11</sup>J. M. Benoit, B. Corraze, S. Lefrant, W. J. Blau, P. Bernier, and O. Chauvet, *Synth. Met.* **121**, 1215 (2001).
- <sup>12</sup>B. J. Landi, R. P. Raffaele, M. J. Heben, J. L. Alleman, W. V. Derveer, and T. Gennett, *Nano Lett.* **2**, 1329 (2002).
- <sup>13</sup>L. J. van der Pauw, *Philips Research Reports* **13**, 1 (1958).
- <sup>14</sup>M. Halik, H. Klauk, U. Zschieschang, G. Schmid, C. Dehm, M. Schütz, S. Mäisch, F. Effenberger, M. Brunnbauer, and F. Stellacci, *Nature (London)* **431**, 963 (2004).
- <sup>15</sup>Q. Cao, Z.-T. Zhu, M. G. Lemaitre, M.-G. Xia, M. Shim, and J. A. Rogers, *Appl. Phys. Lett.* **88**, 113511 (2006).
- <sup>16</sup>M. Shtein, J. Mapel, J. B. Benziger, and S. R. Forrest, *Appl. Phys. Lett.* **81**, 268 (2002).